Heliyon 10 (2024) e29579

Contents lists available at ScienceDirect

Heliyon

journal homepage: www.cell.com/heliyon

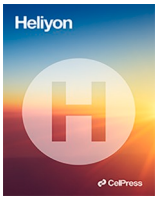

Research article

Multi-loop active disturbance rejection control and PID control strategy for poultry house based on GA, PSO and GWO algorithms

Narjice Elghardouf *, Yassine Ennaciri, Ahmed Elakkary, Nacer Sefiani

Systems Analysis, Information Processing, and Integrated Management Laboratory, Superior School of Technology of Salé, Mohammed V University in Rabat, Morocco

ARTICLE INFO

Keywords:
Active disturbance rejection control and PID
Poultry house system
Climate control
GA
PSO and GWO algorithm
Multi-loop control

ABSTRACT

Maintaining the health and welfare of broilers, besides obtaining and optimizing good performance, are the main objectives of poultry production. In response, climate control remains the most guaranteed strategy for managing livestock successfully. Separate controlling temperature and humidity on the one hand; and contaminant gases on the other was a focus of several investigations. Thus, the particularity of this work which involves the study, analysis, and control of broiler livestock building while taking into account, at the same time, all the system's constituent variables (i.e., temperature, humidity, NH_3 and CO_2 concentration, air velocity, and differential pressure). In this paper, an Active Disturbance Rejection Control (ADRC) and Proportional Integral Derivative (PID) controllers were designed and combined with a multi-loop approach for a multi-inputs multi-outputs (MIMO) system. Then, Genetic Algorithm (GA), Particle Swarm Optimization (PSO), and Grey Wolf Optimization (GWO) were used to obtain the optimal controllers' parameters employing the reward function, the Integrated Time Absolute Error (ITAE), according to the poultry system requirements. Simulation experiments were carried out using the Matlab Simulink toolbox to verify the effectiveness of all the proposed control methods with the two optimization algorithms regarding stabilization and tracking setpoints. Despite the introduction of several disturbances in the plant model, the PSO-ADRC controller still exhibits notable benefits in terms of rise time, overshoot, settling time, and good disturbance rejection, proving the robustness of the suggested control method.

1. Introduction

With the impressive growth of the population and its consumption rate, global demand for poultry meat continues to rise. In response to this high demand, modern livestock breeding is mostly done in enclosed infrastructure with an automated control mode to increase productivity and animal's protection from different perturbations. In fact, farmers and producers of these animals' work on the suitability of these poultry buildings to provide animal welfare, growth, and profitability. The sufficiency of the housed livestock is determined by supplying fresh air, adequate temperature, humidity, lighting [1] and avoiding, particularly, thermal stress. Therefore, the process requires stringent and effective regulation during the rearing period. Firstly, it was essential to create a microclimate environment model to represent and simulate the real environment in the broiler livestock buildings; which reflects the environmental information of each point in the house, such as temperature, humidity, and air velocity; and understand the strong correlation and

* Corresponding author.
E-mail address: Narjice.elghardouf@gmail.com (N. Elghardouf).

https://doi.org/10.1016/j.heliyon.2024.e29579
Received 29 August 2023; Received in revised form 7 December 2023; Accepted 10 April 2024
Available online 14 April 2024

coupling between all these variables. Regulating one of them will also affect the others [2]. Then, applying a suitable automatic controller to guarantee regulation, prediction, stability, safety, and accuracy regarding the setting parameters and rejecting any disturbance throughout the rearing period.

Controlling heating, ventilation, and air conditioning is the principal key to guaranteeing this optimum micro-climate objective. Indeed, this regulation allows for achieving the desired environmental conditions and air quality that all poultry farms seek by lowering the concentrations of harmful gases, and excess heat and humidity produced inside the building. However, improper tuning of these controllable variables may result in a rise in the thermal energy through heating and/or electrical energy consumed by the fans or cooling pads, which their costs have currently climbed. Taking all of these factors into account is challenging, in general.

Based on these foundations, we were successfully interested in modeling and command to analyze the studied system, develop novel control strategies, optimize the tuning parameters, and generate simulations that offer continuous control of temperature, relative humidity, pollutant gases, air velocity, and pressure inside the livestock building; and guarantee efficient risk handling of the poultry house environment. The climate control decision is not only based on the financial profitability of the production activity but also on the choice to increase the satisfaction of consumers who are becoming more and more concerned with product quality, respect animal health and welfare, and reduce energy consumed, greenhouse gases and ammonia emissions which is the cause of many pathologies and environmental problems.

Numerous researchers and strategies have been explored in the literature to control poultry houses. For the purpose of controlling the temperature in broiler livestock buildings, Aborisade and Oladipo [3], Oladayo and Titus [4] developed PID and fuzzy-PID controllers. They discovered that the Fuzzy-PID strategy performed better than the PID controller concerning steady-state error and settling time. With the same objective, three different logic switches (ON-OFF, PID, fuzzy) were created by Refs. [2,5,6]. The fuzzy controller outperforms the other two controllers when comparing comfort performance regarding temperature and humidity, and energy consumption. While Soldatos et al. [7] used a successfully robust nonlinear feedback control with feedforward action to ensure minor deviations in the temperature and humidity, Daskalov et al. [8] confirmed the effectiveness of applying a nonlinear adaptive method for setting the same desired environmental parameters inside any air-conditioning animal building system. Xie et al. [9] established a multi-factor environmental control system based on the fuzzy control theory for swine buildings. The regulation strategy provided a comfortable environment for the growth of pigs regarding temperature, humidity, and NH_3 concentration.

In the field of greenhouse systems, Manonmani et al. [10] engaged in modeling and controlling the infrastructure using artificial neural networks to attain the desired growth conditions, such as humidity and temperature, for higher efficiency. Groener et al. [11], in his turn, designed an environmental open-source control system allowing the decreasing of the cost and size of sensors to automate processes, providing an excellent scientific proposal for further environmental regulation of poultry livestock buildings.

The previously mentioned researches serve as a guide for the brooder buildings regulation. However, the poultry industry is particularly delicate and demands high levels of precision regarding the indoor environment automated control due to the sensitivity of the product. Therefore, the control strategy should be as appropriate as possible to the model despite the ignorance of all the potential perturbations. Due to the PID regulator's limitations in this area and to better regulate the environment for poultry, a new, robust control strategy based on the active rejection of disturbances has been implemented. This control strategy's approach is to predict and adjust all the actual plant's unknown dynamics, disturbances, and parameter uncertainties while requiring the least amount of information [12]. The controller uses the extended state observer (ESO) to treat and reject the internal and external disturbances as total disturbance and a feedback controller to compensate for this existing disturbance and generate the desired signal. The ADRC control has been successfully used with a variety of systems, including control of DC motor [13], wind and power systems [14–16], mechanics [17] and robotics [18]. However, to the authors' knowledge, no literature review work has employed ADRC control to regulate poultry environment building.

Inspired by the numerous advantages of the ADRC controller, a comparative study of PID and ADRC controllers was carried out on the Multi-Input Multi-Output (MIMO) system for the climate control in the livestock building. It is important to note that, within the poultry house, there is a strong dependence and interaction between the microclimatic variables, which are impacted by themselves and the outside climate, necessitating system stabilization to prevent fluctuations and disturbances. To our knowledge, no research work in the literature has employed ADRC controller to regulate poultry environment building, and even at the classical PID level, there is no study dealing with the automation of a complete mathematical poultry house model with all the existing couplings and interactions of all the microclimatic variables (i.e., temperature, humidity, NH_3 and CO_2 concentrations, air velocity, and differential pressure).

The strength of this research lies in the novelty of using a new innovative mathematical model that is complete and validated, which takes into consideration all the environmental variables of the poultry house and the strong interaction that connects them on the one hand and with the external climate on the other, for controlling, stabilizing, and supervising poultry house climate control. Furthermore, the improved method ensured the achievement of reference setpoints and avoidance of undesirable values with a quick rise time, small error, and optimal tuning of the controllable variables (i.e., ventilation rate, heating, and evaporative cooling), which lowers energy consumption and improves animal welfare.

This study provides the literature with a reference for the climate control of the breeding system model for different species under varied climatic conditions and with diverse types of animal livestock structures. The developed approach can also be applied to other MIMO systems with interdependent variables and thus provides relevant and specific recommendations at the level of engineering applications, particularly in poultry farming and production.

The main purpose of this work is to control the environmental factors inside the breeding building according to specific needs, using two control methods. This objective can be achieved through investigating, evaluating, developing adapted control laws (Multi-loop PID and ADRC) and then comparing the performance of each schema for the poultry environment breeding regarding all the multiple

microclimatic environment variables. A mathematical model of six outputs and three inputs is considered, and the original nonlinear system is linearized using the Jacobian linearization approach around the equilibrium point. In order to stabilize the system, reach the reference signals, and reject the disturbances during the breeding period employing these controllers, tunning methods must be applied to increase the performance of the process. Intelligent optimization algorithms are the most commonly studied parameter optimization methods, such as the Ant Colony algorithm, Particle Swarm Optimization (PSO), simulated annealing, and Genetic Algorithm. In this paper, the Genetic Algorithm (GA) heuristic method, PSO and Grey Wolf Optimization (GWO) will be used for tuning the value parameters of the PID and ADRC controllers, which have been tested in the MATLAB/Simulink environment.

The rest of this paper is organized in three parts. The mathematical model used in poultry livestock building is presented in the first section. The theoretical analysis and modeling of the two multi-loop MIMO control strategies (PID and ADRC) are introduced in the second section, along with a description of the GA, PSO and GWO optimization algorithms employed in this work. Finally, these controllers were applied, and the final part displays the simulation results.

2. Mathematical model

The mathematical model for a closed poultry livestock building is expressed according to the previous works [19–21], and [22] as

$$\begin{cases} \dfrac{dT_{in}}{dt} = \dfrac{Q_c - rE_{ev}}{\rho_{air}.V_b.C_p} + \dfrac{N_c.M^{0.75}}{100.\rho_{air}.V_b.C_p}\left(854 - 12.2T_{in} - 0.228T_{in}^2\right) - \left(\dfrac{K_g}{\rho_{air}.V_b.C_p} + \dfrac{D_V}{V_b}\right)(T_{in} - T_{out}) \\ \dfrac{dH_{in}}{dt} = \dfrac{E_{ev}}{\rho_{air}.V_e} + \dfrac{10^{-5}.N_c.M^{0.75}}{\rho_{air}.V_e.h_{vi}}\left(546 - 7,8T_{in} + 0.228T_{in}^2\right) - \dfrac{D_V}{V_e}(H_{in} - H_{out}) \\ \dfrac{dC_{NH3_{in}}}{dt} = \dfrac{31.A.N_c}{24.3600.V_b} - \dfrac{D_V}{V_b}(C_{NH3_{in}} - C_{NH3_{out}}) \\ \dfrac{dC_{CO2_{in}}}{dt} = \dfrac{\rho_{CO_2}.N_C}{V_b.3600}\left(340 - 40.7d + 5.59d^2 - 0.0683d^3\right) - \dfrac{D_V}{V_b}(C_{CO2_{in}} - C_{CO2_{out}}) \\ V_{air} = \sqrt[0.6]{\left|\left(\dfrac{10R_V}{0.081(T_b - T_{int})M^{-0.08} - 10R * m_{coat}} - 5.4\right) * \dfrac{M^{0.13}}{15.7}\right|} \\ \Delta p = \left[0,01 * RH_{int}.e^{\frac{C_1}{T_{int}} + C_2 + C_3T_{int} + C_4T_{int}^2 + C_5T_{int}^3 + C_6\ ln\ T_{int}}\left(1 + \dfrac{0,62198}{H_{int}}\right)\right] - P_{out} \end{cases} \quad (1)$$

In this regard, this work focuses on the dynamical model describing the state space form of the system through differential equations of the state vector; representing the indoor temperature ($x_1 = T_{in}$), humidity ($x_2 = H_{in}$), NH_3 & CO_2 concentrations ($x_3 = C_{NH3_{in}}, x_4 = C_{CO2_{in}}$); and the system's input related to the heating ($u_1 = Q_c$), evaporative cooling ($u_2 = E_{ev},$), and ventilation ($u_3 = D_v$). Air velocity and differential pressure are considered the results of these state variables. The simplified model becomes:

$$\begin{cases} \dot{x}_1 = \dfrac{u_1 - ru_2}{a} + b\left(854 - 12.2x_1 - 0.228{x_1}^2\right) - \left(\dfrac{K_g}{a} + \dfrac{u_3}{V_b}\right)(x_1 - T_{out}) \\ \dot{x}_2 = \dfrac{u_2}{c} + R\left(546 - 7.8x_1 + 0.228{x_1}^2\right) - \dfrac{u_3}{V_e}(x_2 - H_{out}) \\ \dot{x}_3 = R_{NH3} - \dfrac{u_3}{V_b}(x_3 - C_{NH3_{out}}) \\ \dot{x}_4 = R_{CO2} - \dfrac{u_3}{V_b}(x_4 - C_{CO2_{out}}) \end{cases} \quad (2)$$

Where $a = \rho_{air}.V_b.C_p$, $b = \frac{N_c.M^{0.75}}{100.\rho_{air}.V_b.C_p}$, $c = \rho_{air}.V_e$, $R = \frac{10^{-5}.N_c.M^{0.75}}{\rho_{air}.V_e.h_{vi}}$.

$R_{CO2} = \frac{\rho_{CO_2}.N_C}{3600.V_b}\left(340 - 40.7d + 5.59d^2 - 0.0683d^3\right)$, $R_{NH3} = \frac{31.A.N_c}{24.3600.V_b}$.

2.1. Linearization of the model

The Jacobian linearization of the nonlinear system yields the linearization of the dynamic systems (2) around the equilibrium point [23]. The simplified state space form of the linearized model can be computed as follows:

$$\begin{bmatrix} \dot{x_1} \\ \dot{x_2} \\ \dot{x_3} \\ \dot{x_4} \end{bmatrix} = \begin{bmatrix} -\left(12.2b + 0.45b\overline{x_{1e}} + \frac{K_g}{a} + \frac{\overline{u_{3e}}}{V_b}\right) & 0 & 0 & 0 \\ R(-7.8 + 0.45\overline{x_{1e}}) & -\frac{\overline{u_{3e}}}{V_e} & 0 & 0 \\ 0 & 0 & -\frac{-\overline{u_{3e}}}{V_b}0 & 0 - \frac{\overline{u_{3e}}}{V_b} \\ 0 & 0 & & \end{bmatrix} \begin{bmatrix} x_1 \\ x_2 \\ x_3 \\ x_4 \end{bmatrix} + \begin{bmatrix} \frac{1}{a} & -\frac{r}{a} & -\frac{\overline{x_{1e}}}{V_b} \\ 0 & \frac{1}{C} & -\frac{\overline{x_{2e}}}{V_e} \\ 0 & 0 & -\frac{\overline{x_{3e}}}{V_b} \\ 0 & 0 & -\frac{\overline{x_{4e}}}{V_b} \end{bmatrix} \begin{bmatrix} u_1 \\ u_2 \\ u_3 \end{bmatrix}$$

$$+ \begin{bmatrix} \frac{K_g}{a} + \frac{\overline{u_{3e}}}{V_b} & 0 & 0 & 0 \\ 0 & \frac{\overline{u_{3e}}}{V_e} & 0 & 0 \\ 0 & 0 & \frac{\overline{u_{3e}}}{V_b} & 0 \\ 0 & 0 & 0 & \frac{\overline{u_{3e}}}{V_b} \end{bmatrix} \begin{bmatrix} d_1 \\ d_2 \\ d_3 \\ d_4 \end{bmatrix} \tag{3}$$

Therefore, the state space of the model becomes approximately governed by:

$$\begin{cases} \begin{bmatrix} \dot{x_1} \\ \dot{x_2} \\ \dot{x_3} \\ \dot{x_4} \end{bmatrix} = A \begin{bmatrix} x_1 \\ x_2 \\ x_3 \\ x_4 \end{bmatrix} + B \begin{bmatrix} u_1 \\ u_2 \\ u_3 \end{bmatrix} + B_d \begin{bmatrix} d_1 \\ d_2 \\ d_3 \\ d_4 \end{bmatrix} \\ \begin{bmatrix} y_1 \\ y_2 \\ y_3 \\ y_4 \end{bmatrix} = C \begin{bmatrix} x_1 \\ x_2 \\ x_3 \\ x_4 \end{bmatrix} \end{cases} \tag{4}$$

According to the new model (4), the system is characterized in the form of MIMO system (3 × 4), where $A \in R^{4\times4}$ represents the state matrix of the system, $(B, B_d) \in (R^{3\times4}, R^{4\times4})$ represent the input matrix, and the output matrix is $C \in R^{4\times4}$. The state vector is $x \in R^4$.

Where:

$$A = \begin{bmatrix} -\left(12.2b + 0.45b\overline{x_{1e}} + \frac{K_g}{a} + \frac{\overline{u_{3e}}}{V_b}\right) & 0 & 0 & 0 \\ R(-7.8 + 0.45\overline{x_{1e}}) & -\frac{\overline{u_{3e}}}{V_e} & 0 & 0 \\ 0 & 0 & -\frac{\overline{u_{3e}}}{V_b}0 & 0 - \frac{\overline{u_{3e}}}{V_b} \\ 0 & 0 & & \end{bmatrix}$$

$$B = \begin{bmatrix} \frac{1}{a} & -\frac{r}{a} & -\frac{\overline{x_{1e}}}{V_b} \\ 0 & \frac{1}{C} & -\frac{\overline{x_{2e}}}{V_e} \\ 0 & 0 & -\frac{\overline{x_{3e}}}{V_b} \\ 0 & 0 & -\frac{\overline{x_{4e}}}{V_b} \end{bmatrix}, B_d = \begin{bmatrix} \frac{K_g}{a} + \frac{\overline{u_{3e}}}{V_b} & 0 & 0 & 0 \\ 0 & \frac{\overline{u_{3e}}}{V_e} & 0 & 0 \\ 0 & 0 & \frac{\overline{u_{3e}}}{V_b} & 0 \\ 0 & 0 & 0 & \frac{\overline{u_{3e}}}{V_b} \end{bmatrix}, \text{and } C = \begin{bmatrix} 1 & 0 & 0 & 0 \\ 0 & 1 & 0 & 0 \\ 0 & 0 & 1 & 0 \\ 0 & 0 & 0 & 1 \end{bmatrix}$$

2.2. State space to transfer function

The deviation variable form of the linear state space (4) can be represented as:

$$\begin{cases} \dot{X} = AX + BU + B_dD \\ Y = CX \end{cases} \tag{5}$$

By applying the Laplace transform, the general state space model (5) is developed to the corresponding transfer function:

$$\begin{cases} sX(s) = AX(s) + BU(s) + B_dD(s) \\ Y(s) = CX(s) \end{cases} \tag{6}$$

Where $Y(s)$ and $X(s)$ are the Laplace transformation vectors of y and x. equation (6) can also be written in function of the process transfer function matrix G_p and the disturbance transfer function matrix G_d (see Eqs. (7) and (8)):

$$Y(s) = G_p(s)U(s) + G_dD(s) \tag{7}$$

Where:

$$\begin{cases} G_p = C * (sI - A)^{-1} * B \\ G_d = C * (sI - A)^{-1} * B_d \end{cases} \tag{8}$$

2.3. Equilibrium point

We use the following equation (9) to determine the equilibrium point:

$$f(\overline{x},\overline{u}) = 0 \Longrightarrow \begin{bmatrix} \frac{\overline{u_{1e}} - r\overline{u_{2e}}}{a} + b\left(854 - 12.2\overline{x_{1e}} - 0.228\overline{x_{1e}}^2\right) - \left(\frac{K_g}{a} + \frac{\overline{u_{3e}}}{V_b}\right)\overline{x_{1e}} \\ \frac{\overline{u_{2e}}}{c} + R\left(546 - 7.8\overline{x_{1e}} + 0.228\overline{x_{1e}}^2\right) - \frac{\overline{u_{3e}}}{V_e}\overline{x_{2e}} \\ R_{NH3} - \frac{\overline{u_{3e}}}{V_b}\overline{x_{3e}} \\ R_{CO2} - \frac{\overline{u_{3e}}}{V_b}\overline{x_{4e}} \end{bmatrix} = \begin{bmatrix} 0 \\ 0 \\ 0 \\ 0 \end{bmatrix} \tag{9}$$

$$(\overline{x_{1e}},\overline{x_{2e}},\overline{x_{3e}},\overline{x_{4e}}) = \begin{bmatrix} \frac{2.19}{b}\left(\left(12.2b + \frac{K_g}{a} + \frac{\overline{u_{3e}}}{V_b}\right) + \sqrt{\left(12.2b + \frac{K_g}{a} + \frac{\overline{u_{3e}}}{V_b}\right)^2 + 0.91b\left(854b + \frac{\overline{u_{1e}} - r\overline{u_{2e}}}{a}\right)}\right) \\ \frac{V_e}{\overline{u_{3e}}}\left(\frac{\overline{u_{2e}}}{c} + R\left(546 - 7.8\overline{x_{1e}} + 0.228\overline{x_{1e}}^2\right)\right) \\ \frac{V_b.R_{NH3}}{\overline{u_{3e}}} \\ \frac{V_b.R_{CO2}}{\overline{u_{3e}}} \end{bmatrix}$$

3. Control method

Before developing a control strategy, it is essential to consider the stability, controllability and observability of the system. In this study, the system exhibits five real negative poles (−0.00438, −0.00438, −0.00224, −0.00224, −0.00224), which implies that the system is stable. The system controllability and observability were investigating by determining the rank of their matrix as determined as follows:

$$\begin{cases} CTRB = \begin{bmatrix} B & AB & A^2B & A^3B \end{bmatrix} \\ OBSV = \begin{bmatrix} C \\ CA \\ CA^2 \\ CA^3 \end{bmatrix} \end{cases}$$

The matrices have a full rank equal to 4, that is, the rank is exactly the number of states in the state-space model and hence, the system is controllable and observable.

3.1. Relative gain array

The Relative Gain Array (RGA) is a powerful tool for designing control structures and commonly used controllability criteria for determining the ideal pairings for multivariable process control systems and describing the interactions between the manipulated and controlled variables (inputs and outputs). The best RGA is one that is close to the unity matrix [24]. RGA of a nonsingular square complex matrix G is defined in equation (10) below, where $\otimes$ denotes the Schur product (i.e., element by element multiplication):

$$RGA(G) = \Lambda(G) \triangleq G \otimes \left(G^{-1}\right)^{T} = \begin{bmatrix} \lambda_{11} & \lambda_{12} & \cdots & \lambda_{1n} \\ \lambda_{21} & & \ddots & \vdots \\ \vdots & & & \\ \lambda_{n1} & \lambda_{n2} & \cdots & \lambda_{nn} \end{bmatrix} \tag{10}$$

Where λ_{ij} is ij^{th} the relative gain that connect the i^{th} controlled variable with the j^{th} manipulated variable:

$$\lambda_{ij} = \frac{\left(\partial y_i / \partial u_j\right)_{u_k=0, k\neq j}}{\left(\partial y_i / \partial u_j\right)_{y_k=0, k\neq i}} \tag{11}$$

3.2. Multi-loop control strategy

In contrast to the SISO system, where there is no interaction effect, the MIMO process control design is more difficult since each manipulated variable interacts with every other manipulated and controlled variable. As a result, the multiloop controller design is created taking into account all these interactions between the system's variables, by integrating simplified loops that reflect all the existing connections, as shows in Fig. 1. In order to stabilize the industrial poultry house model in the setpoints, the MIMO process with three inputs ($u_1 = Q_c, u_2 = E_{ev}, u_3 = D_v$) and four outputs ($x_1 = T_{int},\ x_2 = H_{int}, x_3 = C_{NH3_{int}},\ x_4 = C_{CO2_{int}}$), disturbed by four parameters ($d_1 = T_{out},\ d_2 = H_{out},\ d_3 = C_{NH3_{out}}, d_4 = C_{CO2_{out}}$), is used to integrate multi-controller configurations. According to Ref. [25], the following is the closed-loop response to the set-point:

$$H(s) = \frac{Y(s)}{Y_{set}(s)} = (I + GG_c)^{-1} GG_c = \frac{1}{D} \begin{pmatrix} \beta_{11} & \cdots & \beta_{14} \\ \vdots & \ddots & \vdots \\ \beta_{41} & \cdots & \beta_{44} \end{pmatrix} \tag{12}$$

Where $H(s)$ is the closed-loop transfer function;

$G = [G_{i,j}; i,j = 1 \ldots 4]$ is the process transfer function;

$G_c = diag\,[G_{c,i}; i = 1, \ldots 4]$ is the multi-loop controller with diagonal elements only;

$Y(s)$ and $Y_{set}(s)$ are the controlled variable and the set-point, respectively.

D is the common denominator of the elements of the transfer function matrix $H(s)$, and which is equivalent of the determinant of the matrix $(I + GG_c)$.

By applying the Routh criterion, the stability of the closed-loop system depends on the characteristic equation (CE) of the denominator D. CE is regarded to specify the value range of the controllers for which the closed-loop system is stable.

In this paper, two regulation strategies based on the combination of the multi-loop schemes with PID and ADRC controllers, were designed to considerably reduce the coupling effect and improve the system stability, as detailed below.

3.3. PID controller

The PID controller (Proportional-Integral-Derivative) is a control system for improving the performance of a closed-loop process. It remains the most widely used controller in industries, despite all the advancements in control over the past 50 years where its correction qualities apply to multiple physical quantities [26]. In order to maintain the process output Y by quickly reaching the system setpoint Y_{set}, the PID reduces the error $\varepsilon(t)$ observed between this setpoint and the direct measurement by three actions: the proportional gain K_p, the integral gain K_i, and the derivative gain K_d, that guarantee the elimination of control deviation errors and the management of rapid process movements, as illustrated in Fig. 2, which encapsulates the parallel type's most often used architecture.

The expression, in the time domain, of the control law is the following:

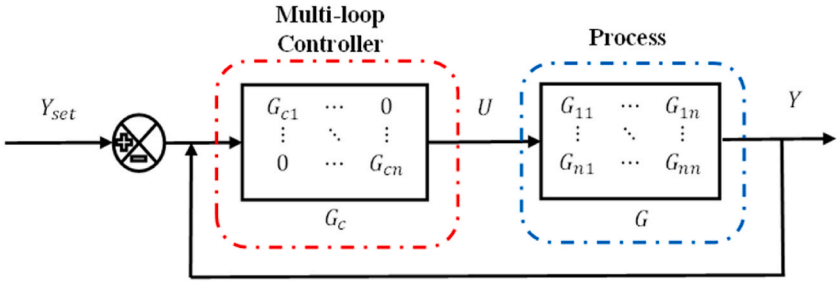

Fig. 1. Block diagram of multi-loop controller for n*n MIMO process.

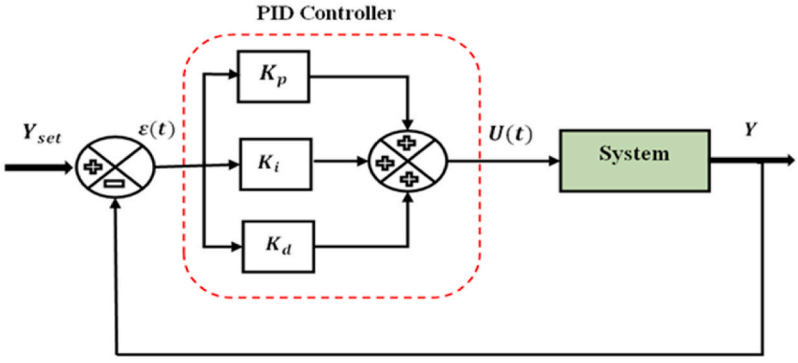

Fig. 2. Block diagram of PID controller.

$$U(t) = K_p.\varepsilon(t) + K_i \int_0^t \varepsilon(\tau).d\tau + K_d \frac{d\varepsilon(t)}{dt} \tag{13}$$

Where $U(t)$ is the control variable and $\varepsilon(t)$ is the difference between the setpoint and the measured output $\varepsilon(t) = Y_{set} - Y$. In the complex domain of the Laplace variable s, where $G_c(s)$ *is* the PID controller transfer function, equation (13) becomes:

$$G_c(s) = K_p + \frac{K_i}{s} + sK_d \tag{14}$$

In order to obtain the best overshoot percentage, settling time, and rise time, the PID parameters have to be adjusted. In this case study, the tunning methods used to adjust K_p, K_i, K_d, are the Genetic Algorithm, PSO, and GWO algorithm.

3.4. ADRC controller

Active disturbance rejection control is a robust control method developed by Han [27], which is based on the principle of estimating and treating both internal (related to modelling uncertainties and measurement noise) and external disturbances (such as the outdoor environment parameters) as a total disturbance of the system in real-time by an extended state observer (ESO) and compensating its effects by a feedback controller [28].

We consider a first order system model of the controlled plant [14]:

$$\dot{y} = f(y, d, t) + b_0 u \tag{15}$$

where y, u and d are respectively the output, input, and external disturbance of the system. $f(y, d, t)$ represent the total disturbance and assumed to be unknow, and b_0 is the gain parameter of the controller. The state space representation of the system is therefore described as [29,30]:

$$\begin{cases} \dot{x}_1 = x_2 + b_0 u \\ \dot{x}_2 = \dot{f} \\ y = x_1 \end{cases} \tag{16}$$

To provide an estimation of the states $x = [x_1, x_2]$, an ESO can be developed with the following form [17,18,31]:

$$\begin{cases} \dot{\widehat{x}}_1 = \widehat{x}_2 + \beta_1 (y - \widehat{x}_1) + b_0 u \\ \dot{\widehat{x}}_2 = \beta_2 (y - \widehat{x}_1) \end{cases} \tag{17}$$

Where $\widehat{x}_1$, $\widehat{x}_2$ provide the estimated values of x_1, x_2, respectively, and $\beta_1 = 2\omega_0$, $\beta_2 = {\omega_0}^2$ are the observer gains values. ω_0 represents the observer bandwidth which can be determined using pole placement technique [32].

The perturbation is eliminated through the control input defined by:

$$u = \frac{u_0 - \widehat{f}}{b_0} \tag{18}$$

In this case, a simple proportional controller (Eq. (19)) with gain value K_p is used to operate the system into the reference signal y_{set}.

$$u_0 = K_p (y_{set} - \widehat{y}) \tag{19}$$

where $K_p = \omega_c$, the desired feedback control gain [33].

The structure diagram of linear ADRC is illustrated in Fig. 3. The parameters that need to be adjusted in ADRC are ω_0, ω_c and b_0. The Genetic Algorithm Optimization, PSO and GWO algorithm are employed in this paper as the tuning strategies to regulate these setting parameters.

4. Algorithm's optimization

4.1. Genetic algorithm

Genetic algorithm is one of the most often used evolutionary optimization methods, which is suitable for many different optimization issues, particularly those involving approximations and modeling uncertainty [34]. Based on a heuristic approach, the GA was developed by John Holland in 1975, which is a method of resolving optimization problems by examining adaptation in both natural and artificial systems [35]. At each stage, the genetic algorithm chooses individuals of the present population to serve as parents and to bear the future generation's offspring. The selection process is based on the individual's adaptability and scores to produce "the most suitable" individual who will pass on their traits and enable the population to evolve into a successful generation [36,37]. Two main rules are applied to produce the next generation from the current one.

- Crossover rules combine two parents to create the next generation's children;
- Mutation rules subject each parent to random modifications to produce children.

The implemented Genetic Algorithm of the poultry house is presented in Fig. 4 flowchart. In our optimization design method, the GA considers the PID and ADRC controllers' parameters adjust (K_p, K_i, K_d,ω_0, ω_c and b_0) as individuals, which are coded, reproduced, and assessed while taking into account the fitness function of each parameter. While creating a new generation, only the selected individuals are combined and the evaluation cycle is repeated until the algorithm delivers the optimal solution to the system with the best fitness function.

4.2. Particle swarm optimization

Particle Swarm Optimization is a population-based stochastic optimization technique developed by Eberhart and Kennedy in 1995, inspired by the social behavior of birds or schools of fish [38]. Since the approach is straightforward and highly effective at searching, the algorithm has been applied in various domains that call for parameter optimization in a high-dimensional space [39].

In the PSO algorithm, a flock of bird is randomly initialized, where each potential solution (bird) is called a particle, which represents one of the parameters to be optimized [40]. At each iteration k, to find the global solution, the individual keeps moving with a velocity that enables them to update their positions. Each particle's speed and position are stochastically adjusted during the repeats to reach the best individual position P_b for each particle and the best global solution G_b for the entire group (swarm). The updated velocity v_i and position x_i of the ith particle are given by Ref. [41]:

$$\begin{cases} x_i(k+1) = x_i(k) + v_i(k+1) \\ v_i(k+1) = \omega.v_i(k) + c_1 r_1 \left(P_{b,i} - x_i(k)\right) + c_2 r_2 (G_b - x_i(k)) \end{cases} \tag{20}$$

Where ω represents the inertia weight of particles. The parameters c_1 and c_2 are known as the cognitive and social coefficients. r_1 and r_2 are two random numbers obtained from a uniform distribution in the range [0, 1]. This process of updating is repeated until a stop

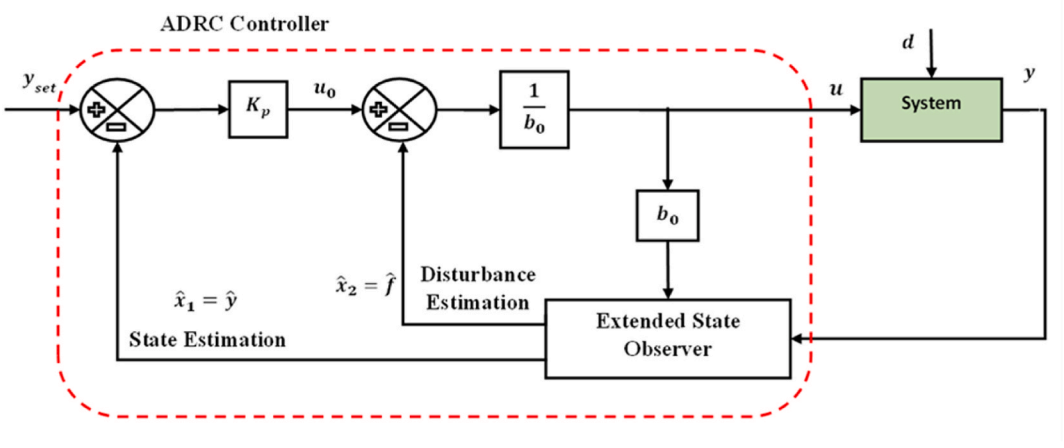

Fig. 3. Structure of ADRC controller.

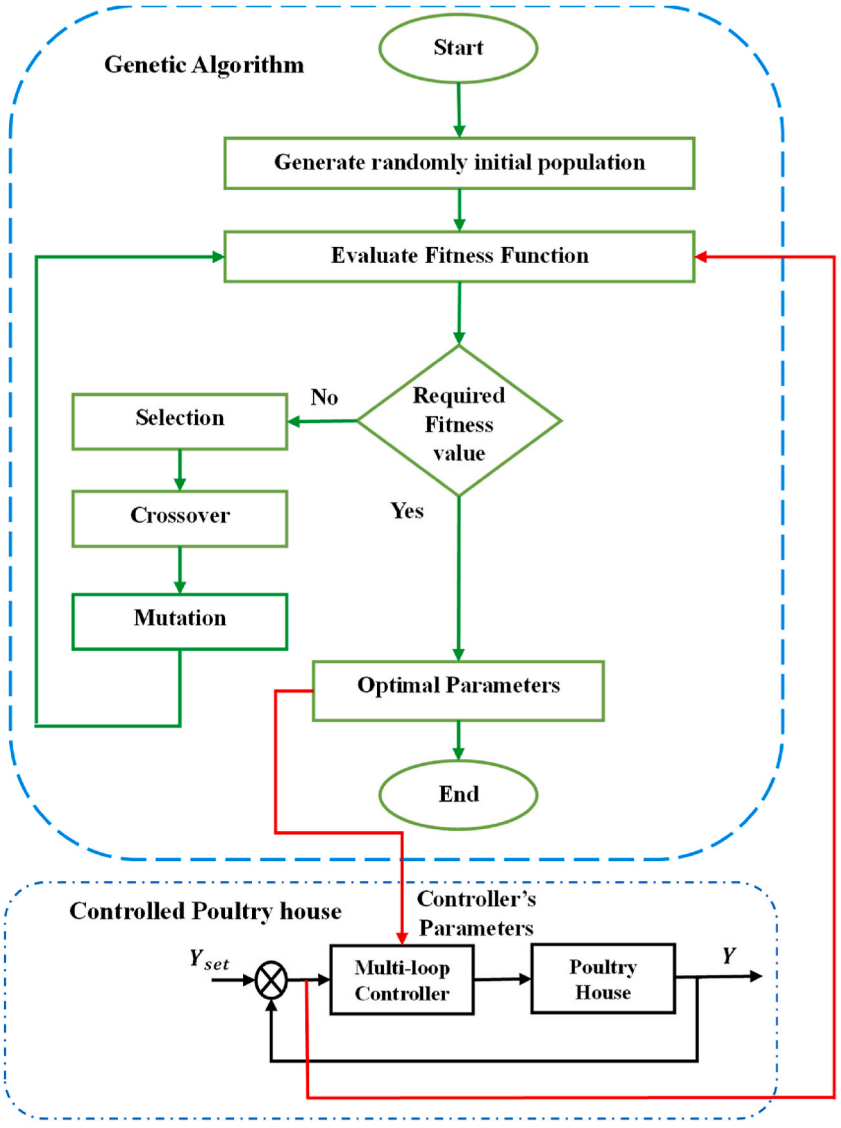

Fig. 4. The proposed functional Genetic Algorithm on the controlled system.

defined condition is satisfied. The flowchart of the designed PSO algorithm applied to the poultry house is shown in Fig. 5. In our case study, the PSO considers the PID and ADRC controller's parameters as the particles to optimize until to find the best personal and global solution according to the fitness function.

4.3. Grey wolf optimization

Grey Wolf Optimization is a new metaheuristic algorithm based principally on the predatory behavior of wild grey wolf groups. Mirjalili et al. [42] introduced this algorithm in 2014, borrowing inspiration from the communal hunting and prey-seeking qualities of grey wolves, in which the group works collectively to optimize their search. The wolf population is classified into four major groups representing the social hierarchical levels (Fig. 6), where each wolf has specific tasks and responsibilities to accomplish through collaboration in the hunting process, which is divided into tracking, chasing, and attacking the prey [43].

The alpha wolves are in the first rank and symbolize the dominant, leading the pack and making decisions such as hunting. Second, beta wolves are regarded as prospective candidates for wolf alpha, helping to make decisions. The third rank is wolf delta, also known as subordinate explorers, responsible for tasks such as scouting and hunting. The omega wolves are the lowest-ranking wolves who keep the wolf pack together and follow the other's orders [44].

During chasing phase, the prey position is defined and the search agents (wolves) adjust continuously their position based on the best solution according to equation (21) below:

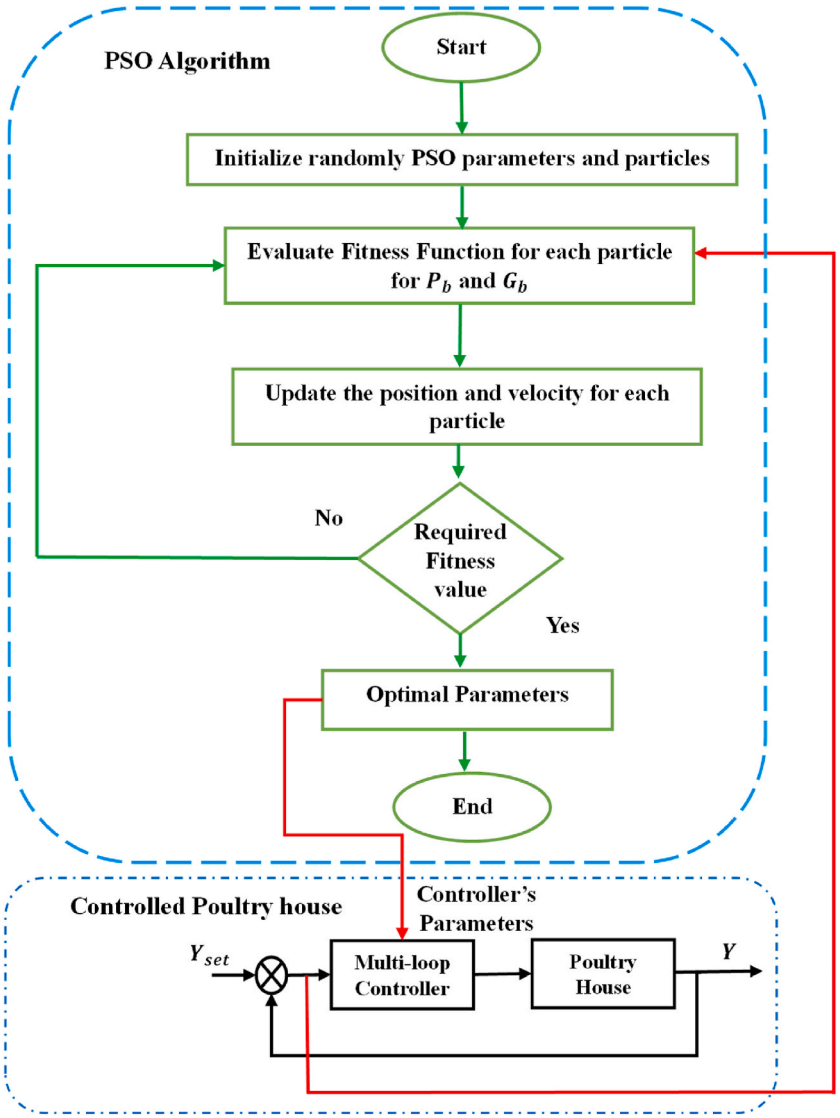

Fig. 5. The designed PSO Algorithm on the controlled system.

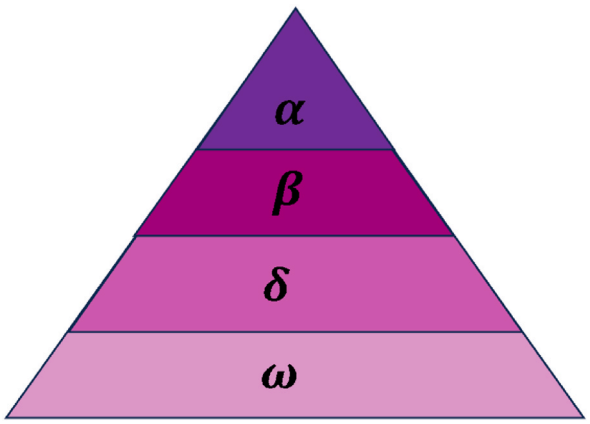

Fig. 6. Hierarchy of grey wolf.

$$\begin{cases} D = \left| C \bullet X_p(t) - X(t) \right| \bullet \omega \\ X(t+1) = X_p(t) - A \bullet D \end{cases} \tag{21}$$

Where D represents the distance between the grey wolf and the prey in the current iteration t, and $X_p(t)$ and $X(t)$ are the prey and wolf's location, respectively. A and C are coefficient vector, computed as:

$$\begin{cases} A = 2a \bullet r_1 - a \\ C = 2 \bullet r_2 \end{cases} \tag{22}$$

Where a is the convergence factor, linearly decreased from 2 to 0 in each iteration, and $[r_1, r_2]$ are random vector between [0,1]. According to the ranks, α, β, δ represent the optimum prey position selected as a guide for other wolves towards prey, and updated several times to adjust the position of omega, according to equation (23):

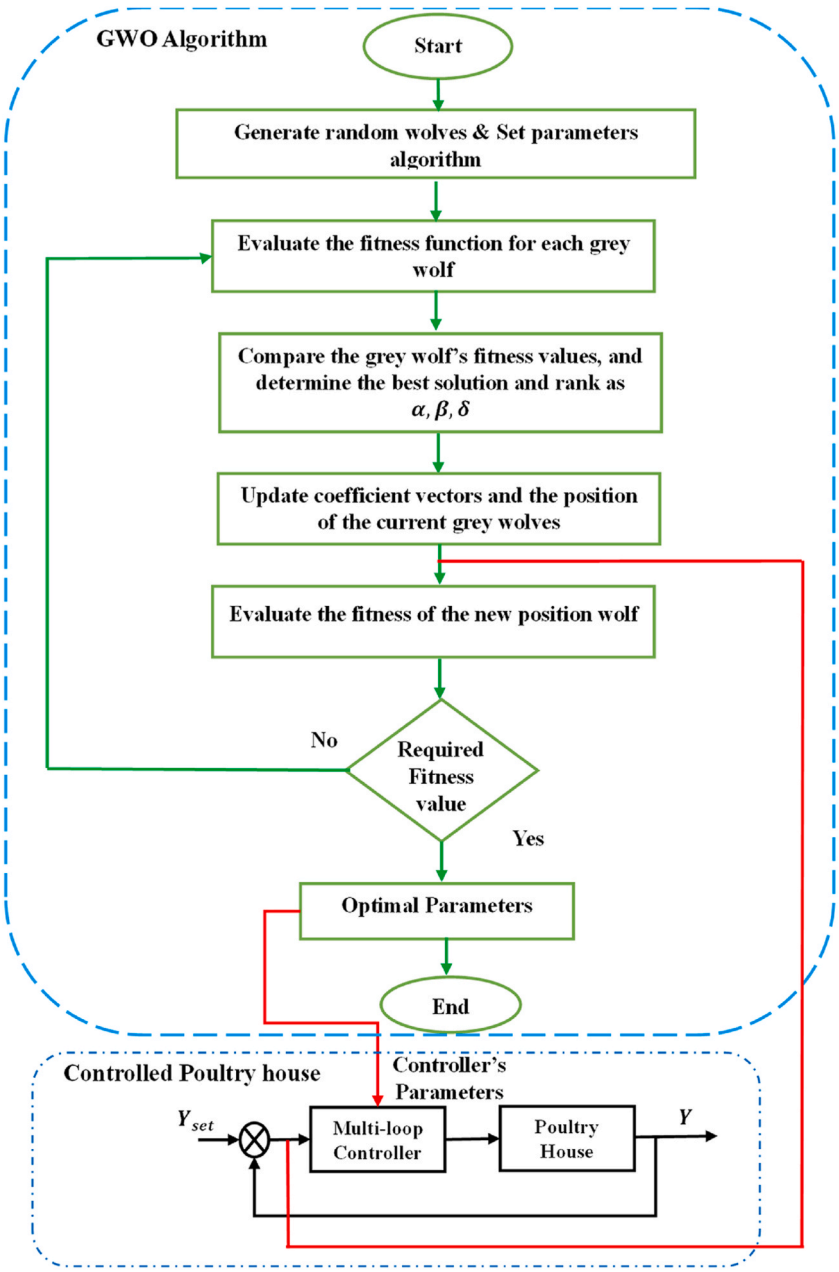

Fig. 7. The designed GWO Algorithm on the controlled system.

$$\begin{cases} D_\alpha = |C_1 \bullet X_\alpha - X| \\ D_\beta = |C_2 \bullet X_\beta - X| \\ D_\delta = |C_3 \bullet X_\delta - X| \end{cases} \tag{23}$$

Where D_α, D_β, and D_δ are the adjusted distance between $\alpha, \beta,$ and δ position to the other wolves, and C_1, C_2, and C_3 are three coefficient vectors obtained using eq. (22). X is the position of other wolf (ω) updated using α, β, δ position (X_α, X_β, X_δ) and coefficient vectors (A_1, A_2, A_3) computed using eq. (22):

$$X(t+1) = \frac{1}{3}\left(|X_\alpha - A_1 \bullet D_\alpha| + |X_\beta - A_2 \bullet D_\beta| + |X_\delta - A_3 \bullet D_\delta|\right) \tag{24}$$

The flowchart of the designed GWO algorithm applied to the poultry house is shown in Fig. 7. In our case study, the GWO considers the PID and ADRC controller's parameters as the wolves' positions to optimize until to find the best solution according to the fitness function.

4.4. Performance evaluation criteria

Tuning the PID and ADRC parameters by GA, PSO and GWO algorithms, requires choosing the best fitness function for optimal results. The specific performance criteria most used in the industry is the Integral Time multiplied by Absolute Error (ITAE). This criterion is applied to the optimization system to determine which values are the most adapted to GA, PSO, and GWO, and will produce the best results for the model poultry house.

The objective function is determined as:

$$ITAE = \sum_0^T t|e(t)| \tag{25}$$

Where $e(t)$ is the error signal in time domain.

5. Simulation results and discussion

5.1. State space model

The actual plant data utilized in the poultry house model was gathered, in the summer season, from a commercial broiler livestock building in the Mediterranean region (Northwest Morocco) with a capacity of 25000 broilers and house dimensions of 120 m in length, 12.4 m in width, and 3,85 m in height (see Fig. 8). The different parameters that were used to simulate and test the suggested controllers are mentioned in Table 1 below.

After calculation, the transfer functions of the poultry house model are determined as:

Fig. 8. The poultry house system.

Table 1
Input parameters used in the mathematical model.

Parameters	Values	Parameters	Values
ρ_{air}	1,2 kg/m^3	K_g	3127 W/°C
ρ_{CO_2}	1,87 kg/m^3	r	0,680 Wh/g
C_p	1006 J/kg K	N_c	25000 (birds)
V_b	3033m^3	V_e	3033m^3
h_{vi}	2,5 0.10^3 kJ/kg	M	0,935 Kg
d	25 (day's number)	A	$d-6$

$$Y(s)=\begin{bmatrix} \frac{2.731*10^{-3}}{s+0.004384} & \frac{-0.0001857}{s+0.004384} & \frac{-0.007583}{s+0.004384} & 0 \\ \frac{-1.4*10^{-13}}{s^2+6.62*10^{-3}\,s+9.83*10^{-6}} & \frac{2.748*10^{-4}\,s+1.205*10^{-6}}{s^2+6.62*10^{-3}\,s+9.83*10^{-6}} & \frac{-3.956*10^{-6}\,s\;-\;1.779*10^{-8}}{s^2+6.62*10^{-3}\,s+9.83*10^{-6}} & 0 \\ 0 & 0 & \frac{-0.002246}{s+0.002242} & 0 \\ 0 & 0 & \frac{-0.002967}{s+0.002242} & 0 \end{bmatrix} U(s)$$

$$+\begin{bmatrix} \frac{0.0031}{s+0.0044} & 0 & 0 & 0 \\ \frac{-1.29*10^{-9}}{s^2+0.0066s+9.8298*10^{-6}} & \frac{0.0022}{s+0.0022} & 0 & 0 \\ 0 & 0 & \frac{0.0022}{s+0.0022} & 0 \\ 0 & 0 & 0 & \frac{0.0022}{s+0.0022} \end{bmatrix} D(s)$$

The relative gain array for the poultry house model is obtained as:

$$RGA=\begin{bmatrix} 1.000001246 & -1.245*10^{-6} & -3.76*10^{-7} & 0 \\ -1.245*10^{-6} & 1.000001245 & -2.76*10^{-8} & 0 \\ 0 & 0 & 0.3642 & 0 \\ 0 & 0 & 0.6357 & 0 \end{bmatrix}$$

According on the findings, we can infer that the system's variables are coupled and interacting. The recommended controller pairing is 1-1/2-2/3-3/4-3, which means using u_1 to control y_1, u_2 to control y_2, and u_3 to control y_3 and y_4.

5.2. Multi-loop control stabilization

The characteristic equation of the poultry house is:

$$CE=(1+G_{c3}G_{33})[(1+G_{c1}G_{11})(1+G_{c2}G_{22})-G_{c1}G_{c2}G_{12}G_{21}]=0$$

After calculation, the equation becomes:

$$CE=a_3s^3+a_2s^2+a_1s+a_0=0$$

With:

$$a_3=2.65*10^4$$

$$a_2=2.4*10^6+7.2\;*10^{-2}G_{c1}+0.72G_{c2}-1.21*10^2G_{c3}$$

$$a_1=2.99+G_{c1}\left(3.22\;*10^{-5}-1.33*10^{-7}G_{c3}+1.98*10^{-5}G_{c2}\right)+G_{c2}\left(4.78*10^{-2}-\;3.36*10^{-2}G_{c3}\right)-0.805G_{c3}$$

$$a_0=5.8*10^{-4}-G_{c3}\left(1.2*10^{-3}+7.4*10^{-8}G_{c1}+1.47*10^{-4}G_{c2}+9.2\;*10^{-9}G_{c1}G_{c2}\right)+G_{c2}\left(7.14*10^{-5}+4.46*10^{-9}G_{c1}\right)+3.36*10^{-8}G_{c1}$$

To satisfy the stability criterion, the parameters of the characteristic equation *CE*, which is a third-order system, must respect the Routh stability conditions:

$a_i > 0, i = \{0, 1, 2, 3\}$ *and* $a_2 a_1 > a_3 a_0$

These conditions will be verified through the optimization algorithms employed in the study.

5.3. Multi-loop PID and ADRC controller schemes responses

Based on the performance indices, the effectiveness of the closed-loop poultry house employing the GA, PSO and GWO algorithms with multi-loop PID and ADRC controllers is examined using MATLAB/Simulink simulations. Table 2 contains a list of the initial parameters that were applied to simulate the GA, PSO, and GWO algorithm, and Fig. 9 represents the Simulink control design of the application of the algorithms to the Multi-loop PID and ADRC controllers.

To verify the effectiveness of the proposed method, we conduct some tests to assess the closed-loop system's tracking performance and disturbance rejection. For the starting simulation, the desired indoor set points and external disturbances were set according to the guidelines based on the birds' age and weight, as shown in Table 3.

The simulation results of the closed-loop response of the indoor temperature, humidity, NH_3 and CO_2 concentrations setting points tuned by the PID and ADRC controllers are illustrated in Figs. 10–13. At t = 100s, the set point for temperature is adjusted from 24 to 27 °C, from 0.0125 to 0.013 $kg_{H2O}/kg_{dry\text{-}air}$ for humidity, from 10 to 7 mg/m^3 for NH_3 concentration, and from 1500 to 1200 mg/m^3 for CO_2 concentration. A step load disturbance was applied at t = 160s of $d_1 = 5$ °C, $d_2 = 0.002$ $kg_{H2O}/kg_{dry\text{-}air}$, $d_3 = 5$ mg/m^3, and $d_4 = 400$ mg/m^3 for the same variables, respectively, to confirm, in addition, the ability of the proposed method to suppress different load disturbances. The time domain specifications, namely the rise time, settling time, and overshoot are employed to evaluate the controller performance for PID and ADRC control using GA, PSO and GWO algorithm. Additionally, the Integral Time multiplied by Absolute Error (ITAE) and the average runtime are used as another set of performance indices to evaluate the most adopted algorithm. The numerical performance measures are listed in Table 4, while the optimal controllers' parameters found are summarized in Table 5.

The dynamic responses for the poultry house applying the three distinct optimization algorithms (GA, PSO, and GWO) are shown in Figs. 10–13. The multiple set points tracking is achieved for the four controlled variables converging as their references. As can be observed, despite the presence of various disturbances (at t = 0s and t = 160s), the proposed methods can still overcome the influence of load disturbances so that the controlled variables quickly stabilize around their setpoints. It can be seen from the partially enlarged view that the PSO-ADRC controller provides a better response for temperature, humidity, and gas concentrations response with a very smooth deviation in tracking the desired set points, and the best disturbance rejection. In fact, the ADRC control strategy performs dynamically better than PID control, the PSO and GWO produced agreeable results when compared to the solutions provided by the GA approach.

As indicated in Table 4, the statistical analysis inferred that the quicker rise time was noticed with the PSO-ADRC at the level of temperature and CO_2 concentration (0.4336s and 0.3036s, respectively), and with the GWO-ADRC at the level of humidity and NH_3 Concentration (2.978s and 0.3046s, correspondingly), and the minimum settling time was recorded with the PSO-ADRC for all the variables (1.4931s for temperature, 4.4130s for humidity, 1.6920s and 1.5026s for NH_3 and CO_2 concentration, respectively) compared to the GA/GWO-ADRC and PID controller system. The minimum overshoot was observed in GA-PID with 0.0042 % for temperature, in PSO-ADRC with 0.0337 % for humidity, and in PSO-PID with 2.7059 % and 1.9432 % for NH_3 and CO_2 concentration, respectively. The ITAE generated by the PSO-ADRC controller has the lower value for temperature with 6.393 (°C) s^2, humidity with 0.458 ($kg_{H2O}/kg_{dry\text{-}air}$).$s^2$, and CO_2 concentration with 10.28 (mg/m^3).s^2. However, the lower ITAE for NH_3 concentration was noted with GWO-ADRC with a value of 3.75 (mg/m^3).s^2. In addition, the GWO algorithm completed the simulation in less time than the GA

Table 2
Input parameters of GA, PSO, and GWO algorithm.

	Parameters	Values
Genetic Algorithm	Generation	250
	Population size	50
	Lower bound	[0 10]
	Upper bound	[100 1000]
	Initial range	[-10 10]
	Selection function	Tournament
	Elite count	0.05* Population size
	Crossover fraction	0.8
	Mutation function	Adaptive feasible
PSO Algorithm	Number of particles for initialization	15
	Maximum Iteration	200
	Lower bound	[0 10]
	Upper bound	[100 1000]
	cognitive and social coefficients (c_1, c_2)	2
	Inertia weight ω	0.5
GWO Algorithm	Population size	50
	Maximum Iteration	200
	Lower search space	[0 10]
	Upper search space	[100 1000]
	convergence factor a	2

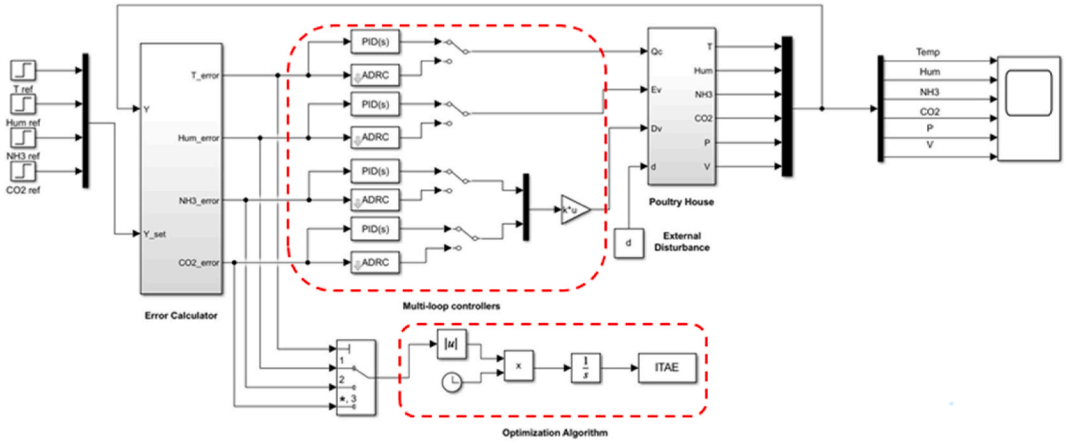

Fig. 9. Simulink presentation of PID and ADRC controllers for poultry house system.

Table 3
Input parameters of set points and disturbances.

Parameters	Set point	Disturbance
Temperature (°C)	24	28
Humidity ratio ($kg_{H2O}/kg_{dry\text{-}air}$)	0.0125	0.014
NH_3Concentration (mg/m^3)	10	1
CO_2 Concentration (mg/m^3)	1500	720

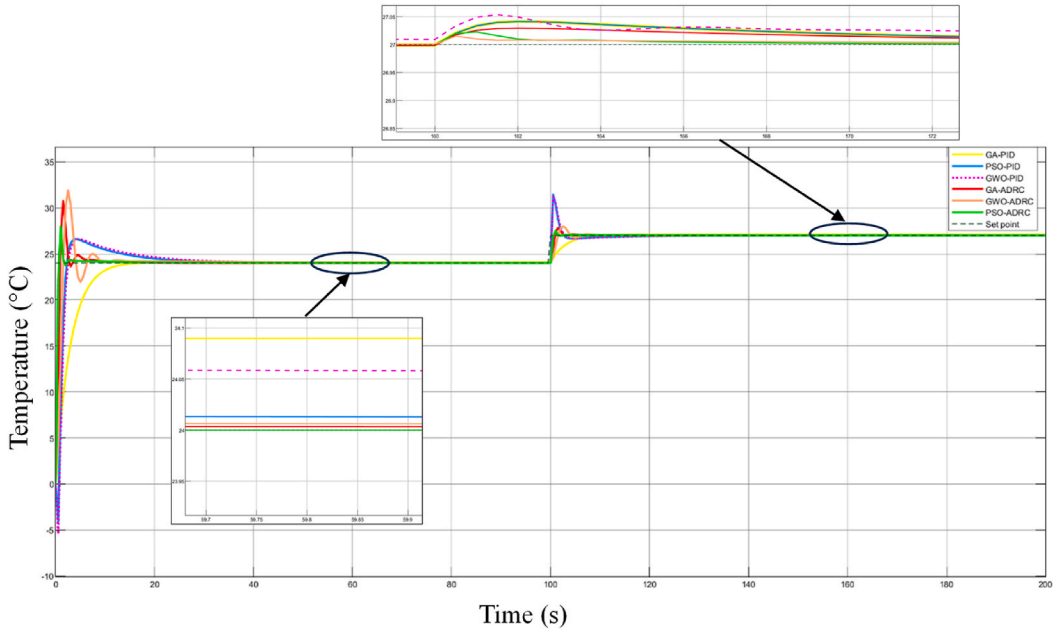

Fig. 10. Dynamic response of temperature with different disturbances.

and PSO algorithms, with an average running time of 4 h and 28 min, compared to 5 h and 34 min for the PSO algorithm and 7 h and 26 min for the GA algorithm. Depending upon all these results, it can be remarked that the PSO-ADRC controller has the least ITAE and the shortest settling time, however, the GWO provides, in general, the faster rise time for both PID and ADRC controllers.

These results are in line with earlier studies that, when a state PID-feedback controller is applied to a temperature-humidity model of broiler house, the settling times for temperature and humidity are 1,49 and 4,37 s, respectively, and the rise times are 1,21 and 3,76 s, for the same variables [45]. Whereas, Daskalov et al. [8] developed a modern control theory based on nonlinear adaptive temperature and humidity control in animal buildings. The method provided fast tracking of different settling values, and guaranteed good

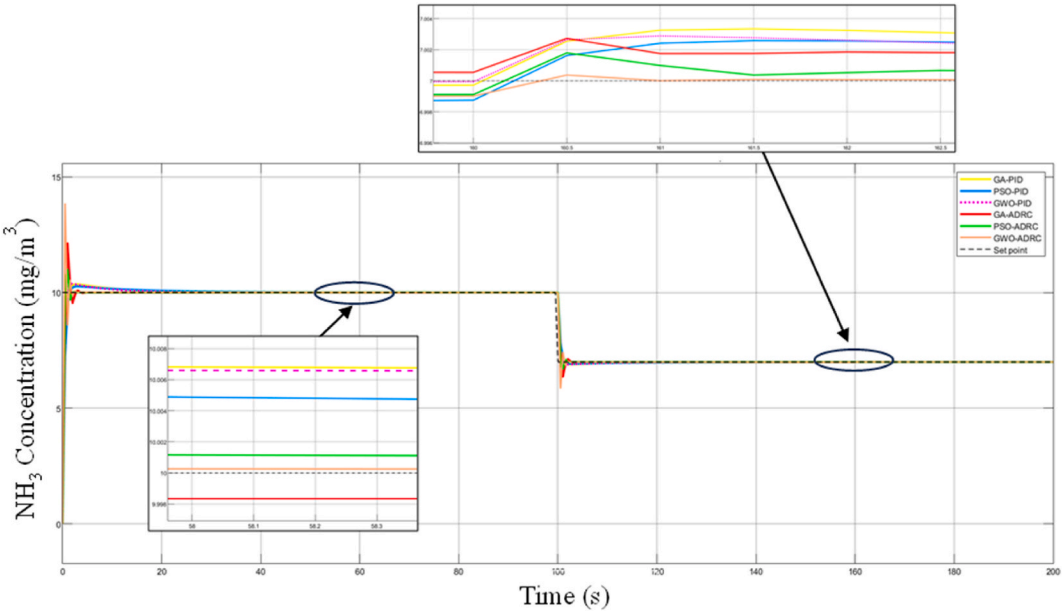

Fig. 11. Dynamic response of NH3 Concentration with different disturbances.

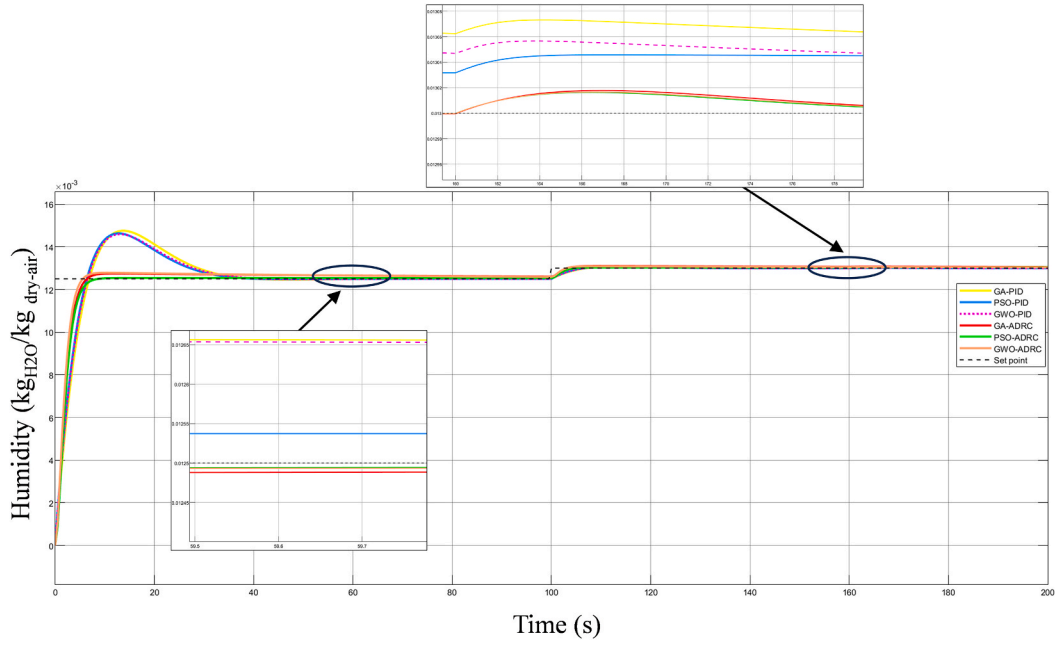

Fig. 12. Dynamic response of humidity with different disturbances.

disturbance rejection with a maximum error less than 0.5 °C for temperature and 0.5 g/kg for humidity.

Using a fuzzy decoupling PID control strategy, an enclosed laying brooder house's temperature and humidity environmental model was controlled, and the findings demonstrate the effectiveness of the fuzzy PID control model over the manual control, with a maximum deviation of 0.5 °C for temperature and 4.93 % for relative humidity between the variable and setpoint [2]. Lahlouh et al. [46], in their turn, carried out a comparative study between a MIMO PID-fuzzy logic, fuzzy logic, and On/Off controllers on a broiler house prototype. The results showed that the PID-fuzzy logic controller is more efficient with a root mean square error of 0.8 °C for temperature and 1.34 % for relative humidity, and a mean value of 2461 ppm and less than 5 ppm for CO_2 and NH_3 concentration. With the same approach, Xie et al. applied a multi-factor fuzzy control in swine building and discovered good results for the indoor temperature and relative humidity, with a maximum relative error of 5 % and 6.3 %, respectively, between the variables and their

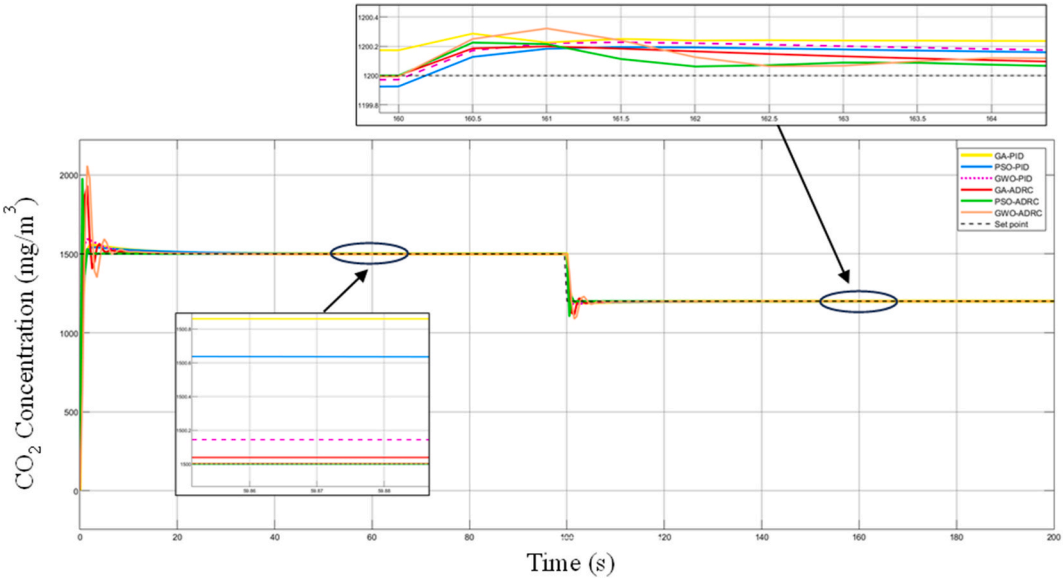

Fig. 13. Dynamic response of CO2 concentration with different disturbances.

Table 4
Comparison of performance indicators of different control methods.

Loop	Controller	Optimization's Method	Rise time	Settling time	Overshoot	ITAE
Temperature	PID	GA	6.6114	11.7839	0.0042	17.55
		PSO	1.1377	20.1745	10.8761	12.08
		GWO	1.0356	20.5672	11.234	15.78
	ADRC	GA	0.7208	5.5433	20.2029	8.24
		PSO	0.4336	1.4931	16.6426	6.393
		GWO	0.7945	7.2365	21.0346	8.567
Humidity	PID	GA	4.7801	30.8756	17.0448	0.611
		PSO	3.4248	27.0652	15.456	0.478
		GWO	3.014	28.685	15.158	0.608
	ADRC	GA	3.2168	5.6404	1.6448	0.573
		PSO	3.0160	4.4130	0.0337	0.458
		GWO	2.978	4.785	1.9678	0.489
NH_3	PID	GA	0.8125	9.5194	3.6380	48.4
		PSO	0.7397	7.4809	2.7059	33.95
		GWO	0.6967	8.245	3.857	44.47
	ADRC	GA	0.5032	2.3625	15.3942	21.58
		PSO	0.3795	1.6920	9.9058	11.86
		GWO	0.3046	1.857	20.576	3.75
CO_2	PID	GA	0.8118	8.9192	3.6697	84.85
		PSO	0.8596	6.3842	1.9432	60.05
		GWO	0.7201	6.0176	5.756	43.745
	ADRC	GA	0.6414	4.6743	28.7542	35.67
		PSO	0.3036	1.5026	31.7637	10.28
		GWO	0.610	7.195	33.56	11.67

setpoints. However, the NH_3 concentration was less than the setpoint (9.1 mg/m3) and ranged from 2 to 3.7 mg/m3 [9]. The selection of fuzzy logic stems mainly from its simplicity of implementation, as it relies just on plant information sources and does not necessitate a mathematical model of the system.

No application has been found for a comparative results overview at the level of the entirety of the six mathematical model variables (i.e., temperature, humidity, gas concentrations, air velocity, and differential pressure) or even at the level of the ADRC controller approach in the field of breeding systems. However, the parameters of the ADRC controller confirm the results of the studies carried out on the ADRC tunning in other areas, which consist of choosing the parameters according to the desired settling time T_s ($\omega_c \approx {}^4/_{T_s}$ and $\omega_0 \approx 3-10\ \omega_c$) [47,48]. Although, the GA algorithm was the closest and the most accurate regarding these two criteria.

In general, PSO and GWO produced similar outcomes in terms of performance; however, the PSO was praised for its convergence speed and precision in reference tracking. The GWO, on the other hand, was distinguished by its speed in terms of global execution procedure and rise time, with the capacity to converge swiftly in comparison to the other algorithms, and the ease of configuration

Table 5
Optimized controllers' parameters.

		Loop 1			Loop 2		
		GA	PSO	GWO	GA	PSO	GWO
PID	K_p	834.76	947.02	968	1000	964.67	896
	K_i	83.758	95.87	92.78	73.447	76.332	95.56
	K_d	0.1785	0.0957	0.124	0.9675	0.1786	0.1056
ADRC	b_0	0.00037	0.000274	0.00027	0.00028	0.0002	0.0002746
	ω_c	0.5002	0.09	0.08	0.90121	0.01	0.013
	ω_0	0.6690	0.9	0.8	0.0014191	0.9	1.012
		Loop 3			Loop 4		
		GA	PSO	GWO	GA	PSO	GWO
PID	K_p	1012.712	984.783	1255.1	1002.01	938.76	1267
	K_i	102.46	74.678	156	95.352	86.823	265
	K_d	0.0657	0.0235	0.0134	0.267	0.1678	0.0965
ADRC	b_0	0.00039	0.00032	0.0003	0.0001648	0.00339	0.00033
	ω_c	0.0012	0.011	0.02	0.0011	0.32603	0.22603
	ω_0	0.8	0.93	1.0023	0.9	0.57518	0.47518

since it required fewer configuration parameters for the optimization process compared to GA and PSO algorithms. Although the GA algorithm takes a longer running time to tune the parameters' controllers and requires more iterations to approximate the optimal solution, its results could be comparable to those of PSO and GWO. Both PSO and GWO deserve consideration in future applications. At the control level, the PID also provides satisfactory results in reference tracking, regulating, and stabilizing. However, the ADRC controller remained more advantageous, especially in disturbance rejection.

The variations in the control signals, namely heating u_1, evaporative cooling u_2, and ventilation rate u_3, are shown in Fig. 14, respectively, indicating the evolution of the manipulated variables throughout the regulation of the controlled outputs. It is observed that both PID and ADRC controllers meet the requirements, although the PSO-ADRC once again outperforms the other schemes. The increased values of evaporative cooling and ventilation rate and nearly no use of the heating meet the recommended measures during the summer season.

The air velocity and differential pressure are the parameters related directly to the environmental variables; they also must be taken under consideration to achieve maximum bird performance and the highest maintenance of the microclimatic conditions below undesirable limit values. Thus, they are considered to be one of the system outputs. The recommended average air speed at this bird age is between 0.4 and 0.7 m/s, while the mean recommended differential pressure inside the poultry house is between 10 and 40 Pa. The response of these variables is obtained from the temperature and humidity model and presented in Fig. 15. The simulation outcomes support the PID and ADRC control model's efficiency again and better satisfy the brood house's requirements for controlling temperature and humidity. Indeed, the airspeed and differential pressure will decrease if we attempt to raise the temperature and humidity inside the building as in the simulation. However, the ADRC controller consistently delivers better performance while maintaining recommended thresholds and converging to the references.

6. Conclusion

In this paper, an analytical study was carried out on the mathematical model relating to a mechanical ventilation broiler house and its micro-environmental variables in the Mediterranean area. Two controller strategies, PID and ADRC, have been developed and tested to control and regulate the indoor climate of the poultry house system based on a multi-loop control configuration since the poultry house is considered as a MIMO system where all the variables are coupled and interacting. Afterward, the metaheuristic approaches Genetic Algorithm (GA), Particle Swarm Optimization (PSO), and Grey Wolf Optimization (GWO) were used to tune and identify the optimal gain parameters of each PID and ADRC controller implemented in each loop of the poultry house system. The different parameters used to simulate and test the proposed controllers are related to the Mediterranean broiler livestock building mentioned under the summer season.

In general, the two control modes with the three optimization approaches were successful in stabilizing, regulating, and controlling the various controlled variables. However, the PSO-ADRC control method dramatically improved dynamic performance with the shortest settling time (1.4931s for temperature, 4.4130s for humidity, 1.6920s and 1.5026s for NH_3 and CO_2 concentration, respectively), and the minimum ITAE for temperature (6.393 (°C) s^2), humidity (0.458 (kg_{H2O}/kg $_{dry\text{-}air}$).s^2), and CO_2 concentration (with 10.28 (mg/m^3).s^2). Whereas, The GWO-ADRC recorder great results in term of rise time, running time of the optimization and small error deviation. In summary, the response curves of the PSO/GWO-ADRC controller, obtained by the simulations performed under different setpoints and step load disturbances, offer the stronger reference tracking and disturbance rejection abilities, improving fast stabilization time, minimal error, and strong robustness.

Consequently, these suggested control strategies can serve as a valuable guide for controlling, adjusting, and stabilizing actual indoor climate poultry house systems. This is especially true given the advantage that the ADRC control approach offers despite all the real plant's unknown dynamics, disturbances, and parameter uncertainties while requiring the least amount of data. This methodology was intended to be applied to other mechanically ventilated animal buildings, including all seasons, and may be expanded to other

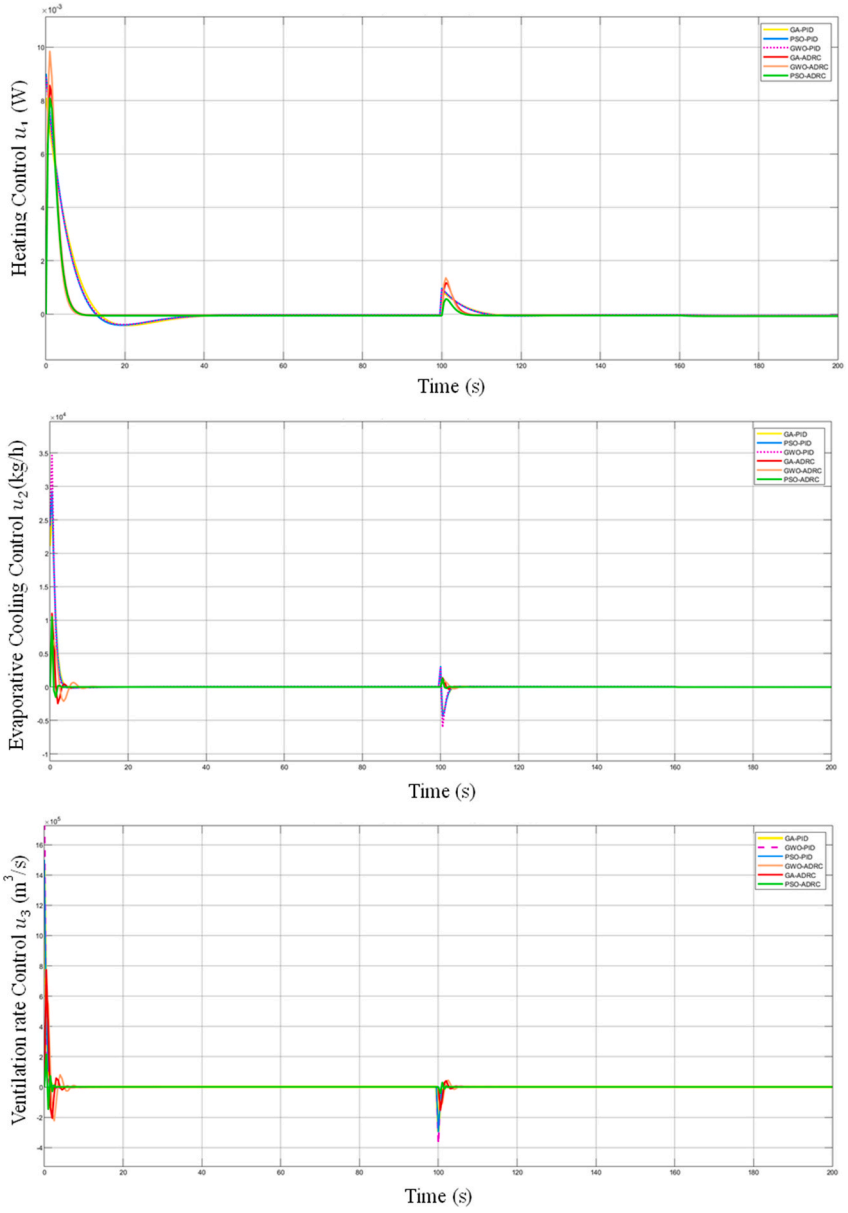

Fig. 14. Manipulated variables' responses.

applications in various fields.

Data availability statement

All data generated or analyzed during this study are included in this published article.

Funding statement

This research did not receive any specific grant from funding agencies in the public, commercial, or not-for-profit sectors.

CRediT authorship contribution statement

Narjice Elghardouf: Conceptualization, Data curation, Formal analysis, Investigation, Methodology, Software, Supervision, Validation, Visualization, Writing – original draft, Writing – review & editing. **Yassine Ennaciri:** Formal analysis, Investigation,

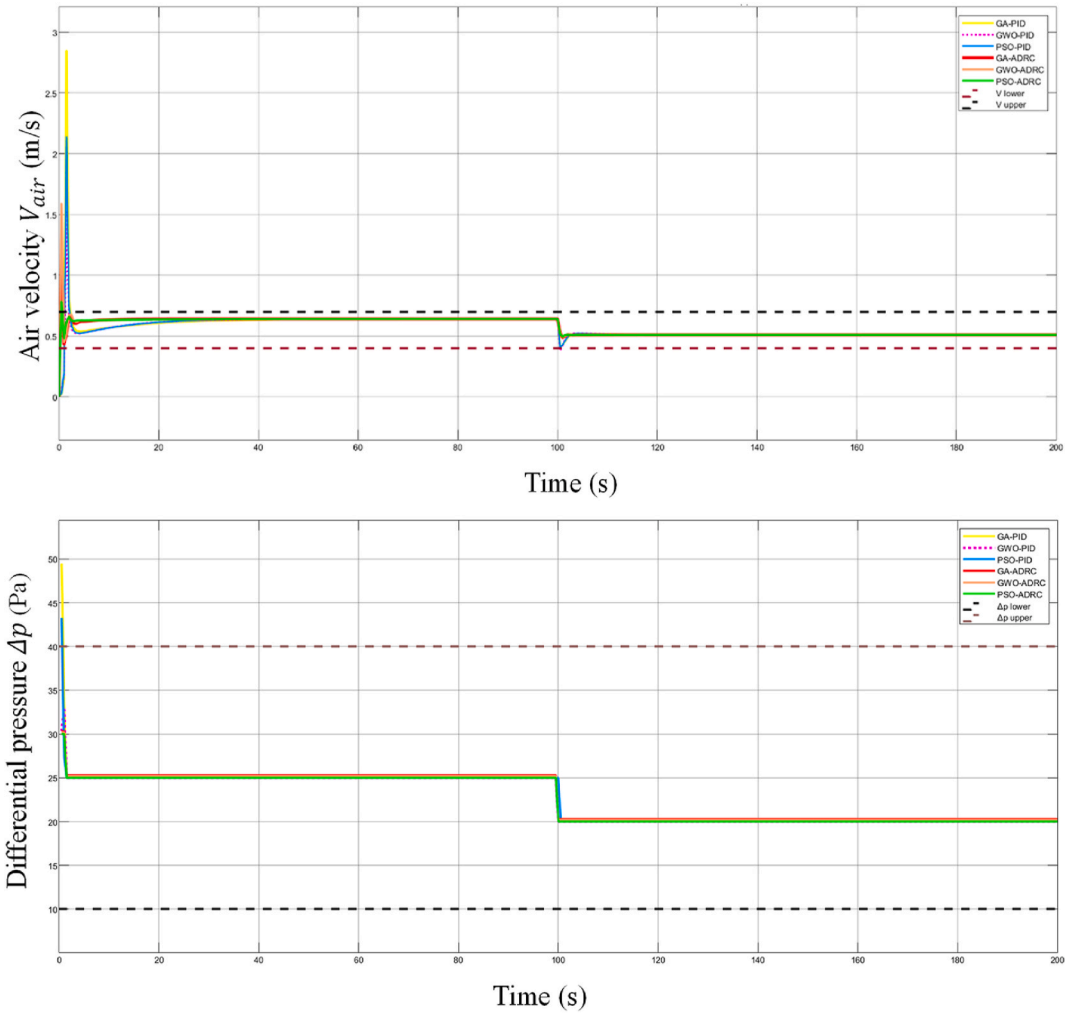

Fig. 15. Air velocity and differential pressure responses.

Software, Supervision, Validation, Visualization. **Ahmed Elakkary:** Project administration, Supervision, Validation, Visualization. **Nacer Sefiani:** Project administration, Supervision, Validation, Visualization.

Declaration of competing interest

The authors declare that they have no known competing financial interests or personal relationships that could have appeared to influence the work reported in this paper.

References

[1] A. Jahedi, , et al.A. Zarei, Evaluation of thermal energy consumption in broiler farms and saving strategies, Arq. Bras. Med. Vet. Zootec. 72 (6) (déc. 2020) 2355–2364, https://doi.org/10.1590/1678-4162-12051.

[2] L. Gao, M. Er, L. Li, P. Wen, Y. Jia, , et al.L. Huo, Microclimate environment model construction and control strategy of enclosed laying brooder house, Poultry Sci. 101 (6) (2022) 101843, https://doi.org/10.1016/j.psj.2022.101843 juin.

[3] D.O. Aborisade, , et al.S. Oladipo, Poultry house temperature control using fuzzy-PID controller, Int. J. Eng. Trends Technol. 11 (6) (mai 2014) 310–314, https://doi.org/10.14445/22315381/IJETT-V11P259.

[4] B.O. Oladayo, A.O. Titus, Pid temperature controller system for poultry house system using fuzzy logic, American Journal of Engineering Research (AJER) 5 (n° 6) (2016) 183–188.

[5] M. Azaza, K. Echaieb, F. Tadeo, E. Fabrizio, A. Iqbal, et A. Mami, Fuzzy decoupling control of greenhouse climate, Arab. J. Sci. Eng. 40 (9) (2015) 2805–2812, https://doi.org/10.1007/s13369-015-1719-5.

[6] G. Ulpiani, M. Borgognoni, A. Romagnoli, , et al.C. Di Perna, Comparing the performance of on/off, PID and fuzzy controllers applied to the heating system of an energy-efficient building, Energy Build. 116 (mars 2016) 1–17, https://doi.org/10.1016/j.enbuild.2015.12.027.

[7] A.G. Soldatos, K.G. Arvanitis, P.I. Daskalov, G.D. Pasgianos, , et al.N.A. Sigrimis, Nonlinear robust temperature–humidity control in livestock buildings, Comput. Electron. Agric. 49 (3) (déc. 2005) 357–376, https://doi.org/10.1016/j.compag.2005.08.008.

[8] P.I. Daskalov, K.G. Arvanitis, G.D. Pasgianos, , et al.N.A. Sigrimis, Non-linear adaptive temperature and humidity control in animal buildings, Biosyst. Eng. 93 (1) (janv. 2006) 1–24, https://doi.org/10.1016/j.biosystemseng.2005.09.006.

[9] Xie Qiuju, Su Zhongbin, Ji-Qin Ni, Zheng Ping, Control system design and control strategy of multiple environmental factors in confined swine building, Trans. Chin. Soc. Agric. Eng. 33 (6) (2017) 163–170.

[10] A. Manonmani, T. Thyagarajan, M. Elango, , et al.S. Sutha, Modelling and control of greenhouse system using neural networks, Trans. Inst. Meas. Control 40 (3) (févr. 2018) 918–929, https://doi.org/10.1177/0142331216670235.

[11] B. Groener, et al., Preliminary design of a Low-cost greenhouse with open-source control systems, Procedia Eng. 107 (2015) 470–479, https://doi.org/10.1016/j.proeng.2015.06.105.

[12] R. Fareh, M. Al-Shabi, M. Bettayeb, , et al.J. Ghommam, Robust active disturbance rejection control for Flexible link manipulator, Robotica 38 (1) (2019) 118–135, https://doi.org/10.1017/S026357471900050X.

[13] J. Yao, Z. Jiao, , et al.D. Ma, Adaptive robust control of DC motors with extended state observer, IEEE Trans. Ind. Electron. 61 (7) (2014) 3630–3637, https://doi.org/10.1109/TIE.2013.2281165.

[14] S. Wang, W. Tan, D. Li, Design of linear ADRC for load frequency control of power systems with wind turbine, in: Proceedings of the 14th International Conference on Control, Automation, Robotics and Vision (ICARCV), Phuket, Thailand, 2016, pp. 1–5, https://doi.org/10.1109/ICARCV.2016.7838795.

[15] H. Laghridat, A. Essadki, M. Annoukoubi, , et al.T. Nasser, A novel adaptive active disturbance rejection control strategy to improve the stability and robustness for a wind turbine using a doubly fed induction generator, J. Electr. Comput. Eng. 2020 (2020) 1–14, https://doi.org/10.1155/2020/9847628, mars.

[16] Y. Zheng, et al., Load frequency active disturbance rejection control for multi-source power system based on soft actor-critic, Energies 14 (16) (2021) 4804, https://doi.org/10.3390/en14164804, août.

[17] F. Hasbullah, , et al.W.F. Faris, Simulation of disturbance rejection control of half-car active suspension system using active disturbance rejection control with decoupling transformation, J. Phys. Conf. Ser. 949 (2017) 012025, https://doi.org/10.1088/1742-6596/949/1/012025.

[18] C.E. Martínez-Ochoa, I.O. Benítez-González, A.O. Cepero-Díaz, J.R. Nuñez-Alvarez, C.G. Miguélez-Machado, , et al.Y.E. Llosas-Albuerne, Active disturbance rejection control for robot manipulator, J. Robot. Control JRC 3 (5) (sept. 2022) 622–632, https://doi.org/10.18196/jrc.v3i5.14791.

[19] I. Lahlouh, A. El Akkary, , et al.N. Sefiani, Mathematical modelling of the hygro-thermal regimeof a poultry livestock building: simulation for spring climate, Int. Rev. Civ. Eng. IRECE 9 (2) (2018) 79–85, https://doi.org/10.15866/irece.v9i2.15132, mars.

[20] A. Costantino, E. Fabrizio, Building design for energy efficient livestock, in: N.M. Holden, M.L. Wolfe, J.A. Ogejo, E.J. Cummins (Eds.), Introduction to Biosystems Engineering, 2020, https://doi.org/10.21061/IntroBiosystemsEngineering/Livestock_Housing_Energy. Housing.

[21] N. Elghardouf, I. Lahlouh, A. Elakkary, , et al.N. Sefiani, Towards modelling, and analysis of differential pressure and air velocity in a mechanical ventilation poultry house: application for hot climates, Heliyon 9 (1) (2023) e12936, https://doi.org/10.1016/j.heliyon.2023.e12936 janv.

[22] N. Elghardouf, I. Lahlouh, A. Elakkary, , et al.N. Sefiani, Mathematical modelling of gas concentrations in commercial broiler houses: simulations and validation in summer season, Int. Rev. Civ. Eng. IRECE 14 (3) (2023) 230, https://doi.org/10.15866/irece.v14i3.21766, mai.

[23] U.C. Berkeley, A. Packard, Jacobian Linearizations, equilibrium points. ME 132, Spring, 2005, pp. 156–177.

[24] M. Ghadrdan, « toward a systematic control design for solid oxide fuel cells, in: Design and Operation of Solid Oxide Fuel Cells, Elsevier, 2020, pp. 217–253, https://doi.org/10.1016/B978-0-12-815253-9.00007-0.

[25] N. Vu Truong, M. Lee, Optimal design of multi-loop PI controllers for enhanced disturbance rejection in multivariable processes, in: Proc. 3rd WSEASIASME Int. Conf. Dyn. Syst. Control, School of Chemical Engineering and Technology Yeungnam University: Gyeoungbuk, Korea, 2007. Available online: http://psdc.yu.ac.kr. (Accessed 15 January 2023).

[26] K.J. Åström, , et al.T. Hägglund, Revisiting the Ziegler–Nichols step response method for PID control, J. Process Control 14 (6) (sept. 2004) 635–650, https://doi.org/10.1016/j.jprocont.2004.01.002.

[27] J. Han, From PID to active disturbance rejection control, IEEE Trans. Ind. Electron. 56 (3) (2009) 900–906, https://doi.org/10.1109/TIE.2008.2011621, mars.

[28] C. Fu, , et al.W. Tan, Tuning of linear ADRC with known plant information, ISA Trans. 65 (nov. 2016) 384–393, https://doi.org/10.1016/j.isatra.2016.06.016.

[29] M. Przybyła, M. Kordasz, R. Madoński, P. Herman, , et al.P. Sauer, Active Disturbance Rejection Control of a 2DOF manipulator with significant modeling uncertainty, Bull. Pol. Acad. Sci. Tech. Sci. 60 (3) (déc. 2012) 509–520, https://doi.org/10.2478/v10175-012-0064-z.

[30] M. Arbaoui, A. Essadki, T. Nasser, , et al.H. Chalawane, Comparative analysis of ADRC & PI controllers used in wind turbine system driving a DFIG, Int. J. Renew. Energy Res (v7i4) (2017), https://doi.org/10.20508/ijrer.v7i4.6270.g7225.

[31] M. Chakib, A. Essadki, , et al.T. Nasser, A comparative study of PI, RST and ADRC control strategies of a doubly fed induction generator based wind energy conversion system, Int. J. Renew. Energy Res (v8i2) (2018), https://doi.org/10.20508/ijrer.v8i2.7645.g7383.

[32] C. Zhao, , et al.D. Li, Control design for the SISO system with the unknown order and the unknown relative degree, ISA Trans. 53 (4) (juill. 2014) 858–872, https://doi.org/10.1016/j.isatra.2013.10.001.

[33] Z. Chu, C. Wu, , et al.N. Sepehri, Active disturbance rejection control applied to high-order systems with parametric uncertainties, Int. J. Control Autom. Syst. 17 (6) (juin 2019) 1483–1493, https://doi.org/10.1007/s12555-018-0509-8.

[34] M. Patrascu, A.B. Hanchevici, , et al.I. Dumitrache, Tuning of PID controllers for non-linear MIMO systems using genetic algorithms, IFAC Proc 44 (1) (2011) 12644–12649, https://doi.org/10.3182/20110828-6-IT-1002.01116.

[35] M.M. Sabir, , et al.J.A. Khan, Optimal design of PID controller for the speed control of DC motor by using metaheuristic techniques, Adv. Artif. Neural Syst. 2014 (déc. 2014) 1–8, https://doi.org/10.1155/2014/126317.

[36] S. Chebli, A. Elakkary, , et al.N. Sefiani, Multi-objective genetic algorithm optimization using PID controller for AQM/TCP networks, Int. Rev. Autom. Control IREACO 10 (1) (2017) 33, https://doi.org/10.15866/ireaco.v10i1.11143, janv.

[37] F. Rerhrhaye, I. Lahlouh, Y. Ennaciri, C. Benzazah, A.E. Akkary, , et al.N. Sefiani, New solar MPPT control technique based on incremental conductance and multi-objective genetic algorithm optimization, Int. J. Energy Convers. IRECON 10 (3) (2022) 70, https://doi.org/10.15866/irecon.v10i3.22156, mai.

[38] J. Kennedy, , et al.R. Eberhart, Particle swarm optimization, Proc. IEEE Int. Conf. Neural Netw. 4 (1995) 1942–1948.

[39] K. Kameyama, « particle swarm optimization-A survey, IEICE Trans. Inf. Syst. E92-D (7) (2009) 1354–1361, https://doi.org/10.1587/transinf.E92.D.1354.

[40] F. Marini, etB, Walczak, Particle swarm optimization (PSO). A tutorial, Chemom. Intell. Lab. Syst. 149 (2015) 153–165, https://doi.org/10.1016/j.chemolab.2015.08.020.

[41] S. Dehuri, , et al.S.-B. Cho, A comprehensive survey on functional link neural networks and an adaptive PSO–BP learning for CFLNN, Neural Comput. Appl. 19 (2) (mars 2010) 187–205, https://doi.org/10.1007/s00521-009-0288-5.

[42] S. Mirjalili, S.M. Mirjalili, et A. Lewis, Grey wolf optimizer, Adv. Eng. Softw. 69 (2014) 46–61, https://doi.org/10.1016/j.advengsoft.2013.12.007, mars.

[43] Y. Hou, H. Gao, Z. Wang, , et al.C. Du, Improved grey wolf optimization algorithm and application, Sensors 22 (10) (2022) 3810, https://doi.org/10.3390/s22103810, mai.

[44] R. Rajakumar, J. Amudhavel, P. Dhavachelvan, , et al.T. Vengattaraman, GWO-LPWSN: grey wolf optimization algorithm for node localization problem in wireless sensor networks, J. Comput. Netw. Commun. 2017 (2017) 1–10, https://doi.org/10.1155/2017/7348141.

[45] I. Lahlouh, A. Elakkary, , et al.N. Sefiani, Design and implementation of state-PID feedback controller for poultry house system: application for winter climate, Adv. Sci. Technol. Eng. Syst. J. 5 (1) (janv. 2020) 135–141, https://doi.org/10.25046/aj050118.

[46] I. Lahlouh, F. Rerhrhaye, A. Elakkary, , et al.N. Sefiani, Experimental implementation of a new multi-input multi-output fuzzy-PID controller in a poultry house system, Heliyon 6 (8) (2020) e04645, https://doi.org/10.1016/j.heliyon.2020.e04645 août.

[47] J. Vincent, et al., On active disturbance rejection-based control design for superconducting RF cavities, Nucl. Instrum. Methods Phys. Res. Sect. Accel. Spectrometers Detect. Assoc. Equip. 643 (1) (juill. 2011) 11–16, https://doi.org/10.1016/j.nima.2011.04.033.

[48] G. Herbst, A simulative study on active disturbance rejection control (ADRC) as a control tool for practitioners, Electronics 2 (4) (2013) 246–279, https://doi.org/10.3390/electronics2030246, août.